Fabrication of Upended Taper-Shaped Cuprous Thiocyanate Arrays on a Copper Surface at Room Temperature

Jiasheng Xu and Dongfeng Xue*

State Key Laboratory of Fine Chemicals, Department of Materials Science and Chemical Engineering, School of Chemical Engineering, Dalian University of Technology, 158 Zhongshan Road, Dalian 116012, P. R. China

Received: February 28, 2006; In Final Form: April 15, 2006

A new strategy has been well designed to form upended taper-shaped cuprous thiocyanate (hereafter abbreviated as CuCNS) arrays on a copper substrate with use of a simple solution-phase method at room temperature. This method consists of a liquid−solid reaction between a solution of thiocyanate ammonium and the copper substrate itself in the assistance of formamide. Novel CuCNS arrays are approximately perpendicular to copper substrate surfaces. Every single crystal shows an upended taper-like morphology (i.e., the tip end points into the surface of copper substrate and the other big end of the taper exposes out, like a dart thrusting into the copper substrate). On the basis of structure and chemical bond analysis, CuCNS crystals tend to grow along the *c*-axis, which is essential for the formation of CuCNS arrays on a copper substrate. This approach also provides a facile strategy to produce different patterns on different copper substrates, which may be applicable to the synthesis of other inorganic materials with various potential applications.

Introduction

In recent years, there has been considerable effort in the fabrication of inorganic materials with novel shapes on various solid substrates, which are essential to the realization of high-performance devices.[1,2] Synthesizing inorganic materials with unusual shapes could therefore be relevant to the design of new types of inorganic materials because the crystal shape dictates the interfacial atomic arrangement of the material. Copper-based compounds are among the most important materials which have been widely used in the area of catalysis, ion exchange, proton conductivity, intercalation chemistry, photochemistry, and chemistry materials. Therefore, much research work has been done in relation to copper-based compounds.[3−6] For instance, Cu_2O with various unique architectures has been manipulatively constructed on Au substrate through an electrochemical crystallization process.[3] Complex 3D dendritic nanoarchitectures of copper hydroxide built up of ultrathin nanosheets have been synthesized in an aqueous solution of formamide on a copper foil substrate.[4] Quasialigned submicrometer CuO ribbons have been successfully synthesized on a copper surface through a simple chemical route involving an oxidation−dehydration process.[5] A series of copper compound materials (including $Cu(OH)_2$ fibers and scrolls, CuO sheets and whiskers, and $Cu_2(OH)CO_3$ rod arrays) have been synthesized on a copper foil by a liquid−solid reaction under alkaline and oxidative conditions at ambient temperature and pressure.[6]

As a transparent wide-gap p-type semiconductor, cuprous thiocyanate CuCNS with its excellent chemical and thermal stability becomes one of the most important functional materials with various applications.[7] For example, CuCNS has been found to photooxidize water in the presence of sacrificial electron acceptors more readily than most photocatalytic materials.[8] It is also an excellent candidate material for application in dye-sensitized solid-state photovoltaic cells due to photographic cyanine dyes being capable of injecting holes into CuCNS with very high efficiencies.[9,10] CuCNS has been used as a material for the synthesis of polymer electrolytes,[11] and has been reported to act as a catalyst for the synthesis of organic compounds.[12] CuCNS usually has been prepared through several different methods, such as the electrodeposition technique,[13] microcrystal growth technology,[14] the alumina template process,[15] and solution reaction.[16] Herein, a new strategy has been successfully designed by employing a liquid−solid reaction between an aqueous solution of NH_4CNS and a copper substrate at room temperature. The copper substrates are used not only as a source of copper but also as a support for CuCNS crystals. The controlled reactions allow the large-scale, template-free, cost-effective synthesis of CuCNS with an ordered, uniform, and stable structure. Especially, CuCNS crystals grow directly on the conducting copper substrate with good electrical contact, which is of crucial importance for the development of a device with high performance.

Experimental Section

The products were prepared on copper substrates by a liquid−solid reaction. Formamide (99.8%) was used without further purification, and a 0.2 M NH_4CNS aqueous solution was freshly prepared. Copper foils (99.9%) with a thickness of 0.12 mm were ultrasonically washed with deionized water before use. In a typical procedure, a piece of copper foil ($10.0 \times 5.0 \times 0.12$ mm^3) was first laid on the bottom of a 20-mL glass vial containing 1.0 mL of formamide and 1.0 mL of NH_4CNS aqueous solution, then the mixed reaction solution was left still at room temperature under atmospheric environment for 1−12 days. The copper foil was then taken out, washed with deionized water and anhydrous ethanol (respectively) several times, and dried in air at 50 °C for more than 5 h. In some cases, copper mesh was also used as a copper substrate and formamide was replaced by an aqueous solution of ammonia ($NH_3 \cdot H_2O$, 25%).

The phase and crystallographic structure of the samples were determined by powder X-ray diffraction (XRD, D/Max 2400,

* Address correspondence to this author. E-mail: dfxue@chem.dlut.edu.cn.

10.1021/jp061274x CCC: $33.50
Published on Web 05/20/2006

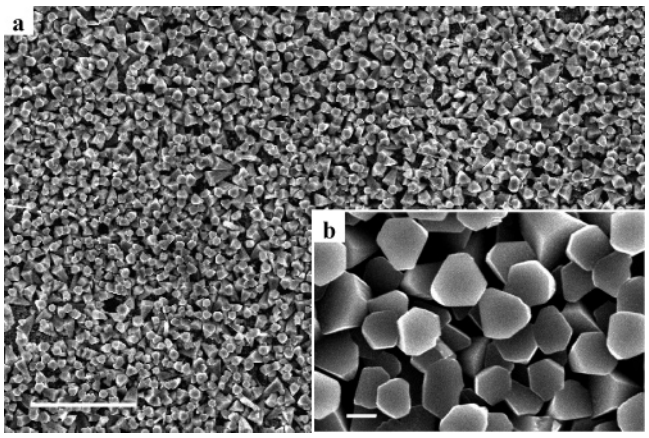

Figure 1. SEM images of cuprous thiocyanate crystals on a copper foil substrate (experimental conditions: 1.0 mL of NH_4CNS (0.2 M) + 1.0 mL of formamide + 3.0 mL of H_2O, at room temperature for 6 days): (a) panoramic morphologies, scale bar = 50 μm; (b) a detailed view in a high magnification, scale bar = 2 μm.

Rigaku, by a diffractometer equipped with the graphite monochromatized Cu Kα radiation). The morphology and size of these crystals were characterized with a scanning electron microscope (SEM, JSM-5600LV, JEOL). UV/vis diffuse reflectance spectra were recorded on a UV−vis−NIR spectrophotometer (JASCO, V-550). FT-IR spectra were recorded on a Fourier transform infrared spectrometry (FT-IR, KBr disk method; NEXUS) at wavenumbers in the range 400−4000 cm^{-1}.

Results and Discussion

The surfaces of all these copper substrates were tarnished (when viewed by the naked eye) after they had been treated in the mixed solution at room temperature. Further examination under an electron microscope indicated that the formation of upended taper-shaped CuCNS crystals is over the entire surface of these substrates, which covered a large area of the copper substrate uniformly and compactly. Figure 1a clearly shows a large-area array of CuCNS grown on a copper foil substrate. The whole substrate surface was successfully covered with uniform and dense arrays of upended taper-like CuCNS, which are approximately perpendicular to the substrate surface. When copper mesh is used as a copper substrate, CuCNS crystals with a similar morphology can be obtained on the copper mesh substrate, as shown in Figure 2. It is clear that every single crystal shows an upended taper-like morphology (Figure 2d). Every tip end points into the surface of copper substrate and the other big end of the taper exposes out, like a dart thrusting into the copper substrate.

When the concentration of mixed solution is low, sparse CuCNS crystals can still be obtained on the surface of the copper mesh substrate with a random arrangement, as shown in Figure S5 (see the Supporting Information). Note that the crystals are better aligned on the copper substrate under high concentration than those under low concentration (comparing Figure 2 to Figure S5). This indicates that the crystal alignment is caused by the space-limited growth. Under low concentration, growth can explore all directions on the copper surface. However, under high concentration, the growth of tilted crystals is more likely to be hindered, whereas the upright crystals grow unabated. An interesting finding (a hollow structure viewed from the top of CuCNS crystal in some of the CuCNS crystals) appeared when CuCNS single crystals were further magnified, as shown in

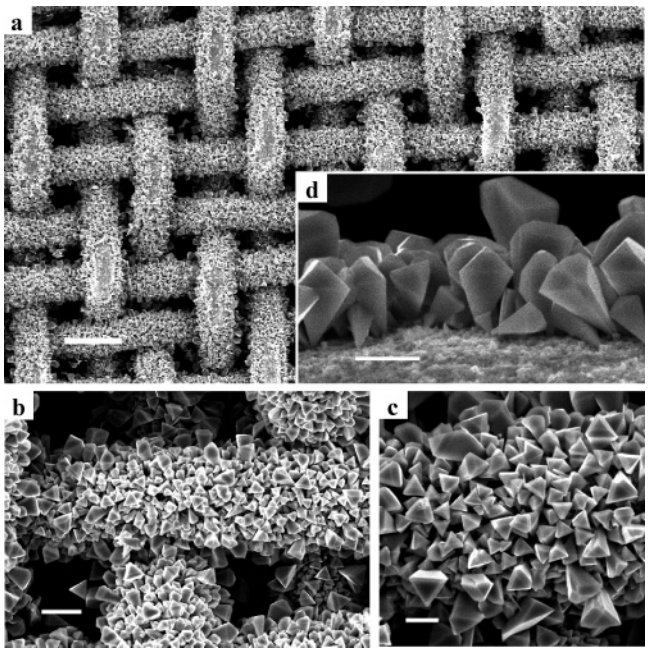

Figure 2. SEM images of cuprous thiocyanate crystals on a copper mesh substrate (experimental conditions: 1.0 mL of NH_4CNS (0.2 M) + 1.0 mL of formamide + 3.0 mL of H_2O, at room temperature for 6 days): (a) panoramic morphologies, scale bar = 100 μm; (b, c) detailed views at different places of copper mesh substrate, scale bar = 20 and 10 μm, respectively; (d) side view on a single Cu wire, scale bar = 5 μm.

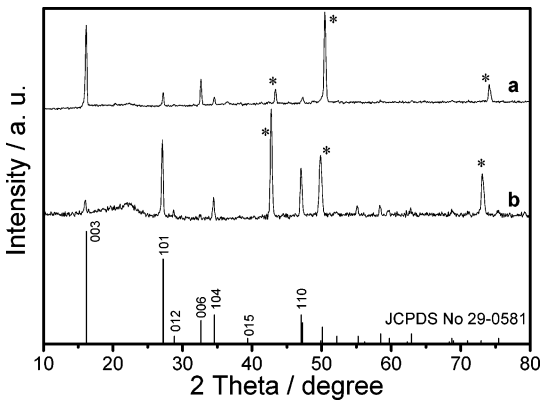

Figure 3. XRD patterns of cuprous thiocyanate crystals on different copper substrates: (a) on a copper foil substrate (SEM images correspond to Figure 1) and (b) on a copper mesh substrate (SEM images correspond to Figure S5, Supporting Information). The standard diffraction pattern of β-CuCNS (JCPDS card File No. 29-0581) is shown as a reference, and reflections generated by the Cu substrate are marked with an asterisk.

Figure S5 (Supporting Information). It is likely that the open structures were formed during the crystallization of CuCNS in the assistance of formamide at a low precursor supersaturation level.

CuCNS exists in two polymorphic forms, α and β, where the β form is commonly available and more stable.[17] β-CuCNS has a hexagonal crystal structure where layers of CNS ions separate Cu cation planes and strong Cu−S bonds three-dimensionally interconnect these layers (as shown in the crystallographic structure of Figures S1−S4, see the Supporting Information). XRD patterns of the as-prepared samples are shown in Figure 3, and all diffraction peaks can be well indexed to the trigonal-phase β-CuCNS (space group *R*3*m*, No. 160), except those marked with asterisks from the copper substrate. Compared with the standard diffraction patterns (JCPDS card

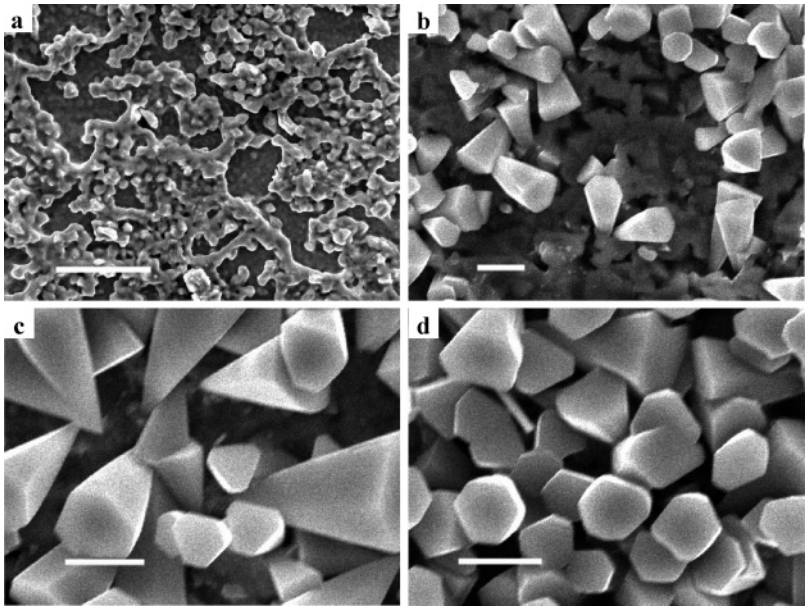

Figure 4. SEM images of cuprous thiocyanate arrays on a copper foil substrate prepared at different reaction stages (experimental conditions: 1.0 mL of NH_4CNS (0.2 M) + 1.0 mL of formamide + 3.0 mL of H_2O): (a) aging at room temperature for 1 day, scale bar = 50 μm; (b) aging at room temperature for 2 days, scale bar = 5 μm; (c) aging at room temperature for 3 days, scale bar = 5 μm; (d) aging at room temperature for 6 days, scale bar = 5 μm.

File No. 29-0581), no characteristic peaks from other phases or impurities can be observed, indicating a high purity and crystallinity of the final products. The phase composition is further supported by FT-IR spectra, as shown in Figure S8 (Supporting Information). The relative intensities of peaks in Figures 3a and 3b are obviously different. The relative intensities of (003), (006), (101), and (110) planes provide information regarding the crystal orientation against the copper substrate, since the powder diffractometer collects reflections only from the crystallographic planes parallel to the substrate (which was used to prepare XRD samples). For example, the XRD pattern of Figure 3a shows the strong intensities of (003) and (006) planes compared to Figure 3b, since alomost all upended tape-shaped CuCNS arrays are approximately perpendicular to the copper foil substrate surface (SEM images are shown in Figure 1). However, Figure 3b shows the strong intensities of (101) and (110) planes but weak intensities of (003) and (006) planes. The observed intensitis of XRD peaks indicate that the elongated direction of taper-like shaped thiocyanate crystals is along the *c*-axis.

Generally speaking, the natural oxidation of copper metal naturally dissolving oxygen in water is very slow due to the surface oxide layer. However, in the presence of formamide, this spontaneous oxidation reaction can be accelerated drastically, which has been widely investigated in previous reports.[4,18] In the presence of an aqueous solution of NH_4CNS, copper can form Cu^+ and react easily with CNS^- to form CuCNS crystals on the surface of copper substrates. The formation processes of the arrays prepared at different reaction stages are respectively studied by SEM measurements, as shown in Figure 4. The growth procedure can be described as follows: at the beginning of the reaction, 1D nuclei started and gradually formed into a large quantity of CuCNS taper-like "roots" on the copper surface first, which served as the nuclei for the crystal growth. The growth of CuCNS crystals stemmed from these "roots" and continued to grow into arrays with reaction proceeding. In this period a typical dissolution−crystallization state was established under the current experimental conditions.

Meanwhile, it should be noted that the heterogeneous nucleation and growth is dominant during the formation of upended taper-shaped CuCNS crystals, because corresponding homogeneous nucleation and growth in solution were not observed. Heterogeneous nucleation on the substrate is promoted over homogeneous precipitation in solution by controlling the precursor supersaturation levels and the interfacial energy between the substrate and the new phase to be formed.[2e] In the current synthetic system, without surface modification, the free energy of crystallization of CuCNS on the copper substrate interface must be intrinsically low enough to relive the supersaturation and induce direct film growth. XRD patterns show that the as-prepared CuCNS crystals grow along the *c*-axis, which is mainly due to the intrinsic CuCNS crystal growth habit.

As shown in Figures S1−S4 (Supporting Information), the β-CuCNS structure is composed of {001} layers of closest-packed cylinders of CuCNS units. High site symmetry in β-CuCNS causes the angles to be very regular. The N−C−S and Cu−N−C sequences are strictly linear; two independent angles at Cu and S are nearly tetrahedral (109.5°). There are two types of bonds in the β-CuCNS crystal lattice: type I, C−N and C−S bonds that are formed before the crystallization, and type II, Cu−S and Cu−N bonds that are formed during the crystallization process on the copper surface. Type II bonds have an essential effect on the crystallization and then determine the final crystal morphology. Cu−N bonds (1.923 Å) are parallel to the *c*-axis symmetrically, and the bond strength is 0.302 vu (the bond strength is quantitatively calculated by the bond-valence model,[19,20] valence unit is abbreviated as vu). Cu−S bonds (2.342 Å) interconnect {001} layers, and the bond strength is 0.238 vu. It is clear that the bond strength along the *c*-axis is stronger than that along other directions in the β-CuCNS crystal lattice. The β-CuCNS crystal therefore prefers to grow along the *c*-axis (the growth rate is determined by the bond number and the bond strength, which formed during the crystallization).

The aqueous solution of ammonia has a similar function with formamide. There have been many reports on the synthesis of

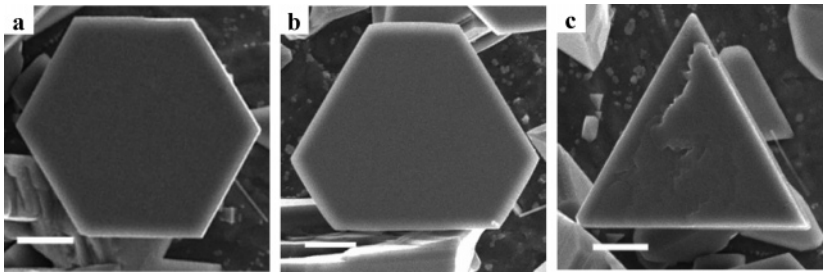

Figure 5. SEM images of cuprous thiocyanate crystals with a shape evolution: (a−c) evolution from the hexagon to trigon, scale bar = 10 μm (experimental conditions: 1.0 mL of NH_4CNS (0.2 M) + 1.0 mL of aqueous solution of ammonia + 3.0 mL of H_2O, at room temperature for 3 days).

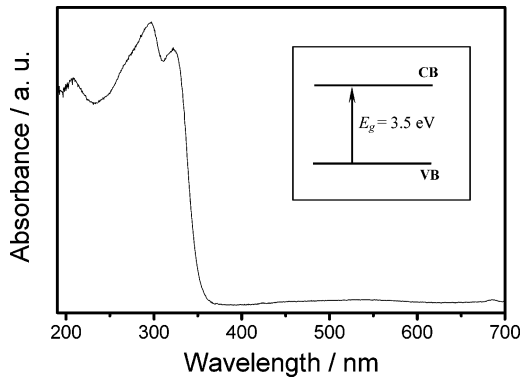

Figure 6. UV/vis diffuse reflectance spectra of the as-prepared β-CuCNS samples. The inset shows the energy level structure (VB refers to the valence band; CB refers to the conduction band).

copper compound materials on a copper foil by a simple liquid−solid reaction under alkaline (aqueous solution of ammonia) conditions.[6] In the current synthetic condition, different shapes of CuCNS can be obtained on the copper substrate, as shown in Figure 5. It may be helpful for us to understand the crystal growth habit of CuCNS. The shape evolution of CuCNS (i.e., from the hexagon to trigon) has been shown in Figure 5, parts a−c, which correspond to the crystal structure of CuCNS from the *c*-axis view (Figure S4, see the Supporting Information). It is well-known that both intrinsic and extrinsic factors (i.e., the crystal structure and growth environment) have significant effects on the final crystal morphology.[20] On the basis of structure and chemical bond analysis, β-CuCNS crystals tend to grow along the *c*-axis, which is essential for the formation of β-CuCNS arrays on the copper surface. The crystal growth environments also have a significant effect on the final morphology. The existence of formamide or ammonia is very important for the formation of β-CuCNS crystals in the current synthetic condition. The default experiments (in the absence of formamide or ammonia) have been employed for evaluating the role of formamide or ammonia in crystal growth. As shown in Figures S6 and S7 (Supporting Information), only some irregular particles are formed on the surface of mesh copper substrate. Therefore, the existence of formamide (or ammonia) plays an important role during the whole crystallization process.

β-CuCNS possesses a steep absorption edge in the UV region as shown in Figure 6. The band gap of β-CuCNS was estimated to be 3.5 eV from the onset of the absorption (λ_{onset} = 352 nm, $E_g = 1241/\lambda_{onset}$).[21] A significant increase in the absorption wavelengths lower than about 352 nm can be assigned to the intrinsic band gap absorption of β-CuCNS. It is clear that the as-prepared CuCNS is a wide-band-gap semiconductor and photosensitive material, and grows on the conducting copper substrate (good electrical contact) directly, which can be easily integrated into devices and may be helpful in the design of new types of photovoltaic devices and materials.

Conclusions

In summary, a new strategy has been designed to form upended taper-shaped CuCNS arrays on a copper substrate by using a solution-phase method at room temperature. Novel CuCNS arrays are approximately perpendicular to copper substrate surfaces. Every single crystal shows an upended taper-like morphology (i.e., the tip end points into the surface of the copper substrate and the other big end of the taper exposes out, like a dart thrusting into the copper substrate). The advantages of our method for the preparation of inorganic materials lie in its simplicity, large-scale, template-free, mild reaction conditions, and the ability to produce different patterns on different copper substrates. The versatile fabrication method demonstrated herein provides not only valuable information for the formation of CuCNS crystal arrays on a copper surface but also builds a foundation for the study of directed crystal growth of various semiconducting crystals on a conducting substrate. In addition, CuCNS crystals grow directly on the conducting copper substrate with good electrical contact, which can be easily integrated into devices. These systems will be useful for a broad range of applications such as sensors, optoelectronics, and catalysis.

Acknowledgment. The authors gratefully acknowledge the financial support of a Program for New Century Excellent Talents in University (NCET-05-0278), the National Natural Science Foundation of China (NSFC No. 20471012), a Foundation for the Author of National Excellent Doctoral Dissertation of P. R. China (FANEDD No. 200322), the Research Fund for the Doctoral Program of Higher Education (RFDP No. 20040141004), and the Scientific Research Foundation for the Returned Overseas Chinese Scholars, State Education Ministry.

Supporting Information Available: SEM and FT-IR results of the reported samples and the crystal structure of CuCNS. This material is available free of charge via the Internet at http://pubs.acs.org.

References and Notes

(1) (a) Murray, C. B.; Kagan, C. R.; Bawendi, M. G. *Science* **1995**, *270*, 1335. (b) Sun, T.; Feng, L.; Gao, X.; Jiang, L. *Acc. Chem. Res.* **2005**, *38*, 644. (c) Mann, S. *Angew. Chem., Int. Ed.* **2000**, *39*, 3392. (d) Colfen, H.; Antonietti, M. *Angew. Chem., Int. Ed.* **2005**, *44*, 5576. (e) Sounart, T. L.; Liu, J.; Voigt, J. A.; Hsu, J. W. P.; Spoerke, E. D.; Tian, Z.; Jiang, Y. *Adv. Funct. Mater.* **2006**, *16*, 335. (f) Vayssieres, L.; Keis, K.; Hagfeldt, A.; Lindquist, S. E. *Chem. Mater.* **2001**, *13*, 4395.

(2) (a) Soulantica, K.; Maisonnat, A.; Fromen, M. C.; Casanove, M. J.; Lecante, P.; Chaudret, B. *Angew. Chem., Int. Ed.* **2001**, *40*, 448. (b) Brown, L. O.; Hutchison, J. E. *J. Am. Chem. Soc.* **1999**, *121*, 882. (c) Yang,

H. G.; Zeng, H. C. *J. Phys. Chem. B* **2004**, *108*, 819. (d) Rodriguez-Clemente, R.; Serna, C. J.; Ocana, M.; Matijevic, E. *J. Cryst. Growth* **1994**, *143*, 277. (e) Bunker, B. C.; Rieke, P. C.; Tarasevich, B. J.; Campbell, A. A.; Fryxell, G. E.; Graff, G. L.; Song, L.; Liu, J.; Virden, J. W. *Science* **1994**, *264*, 48.

(3) (a) Siegfried, M. J.; Choi, K. S. *Adv. Mater.* **2004**, *16*, 1743. (b) Siegfried, M. J.; Choi, K. S. *Angew. Chem., Int. Ed.* **2005**, *44*, 3218.

(4) Zhang, Z.; Shao, X.; Yu, H.; Wang, Y.; Han, M. *Chem. Mater.* **2005**, *17*, 332.

(5) Hou, H.; Xie, Y.; Li, Q. *Cryst. Growth Des.* **2005**, *5*, 201.

(6) (a) Wen, X.; Zhang, W.; Yang, S. *Langmuir* **2003**, *19*, 5898. (b) Zhang, W.; Wen, X.; Yang, S. *Inorg. Chem.* **2003**, *42*, 5005.

(7) (a) O'Regan, B.; Scully, S.; Mayer, A. C. *J. Phys. Chem. B* **2005**, *109*, 4616. (b) O'Regan, B.; Lenzmann, F.; Muis, R.; Wienke, J. *Chem. Mater.* **2002**, *14*, 5023. (c) Perea, V. P. S.; Pitigala, P. K. D. D. P.; Jayaweera, P. V. V.; Bandaranayake, K. M. P. *J. Phys. Chem. B* **2003**, *107*, 13758. (d) Tennakone, K.; Kumara, G. R. R. A.; Kottegoda, I. R. M.; Perea, V. P. S.; Weerasundara, P. S. R. S. *J. Photochem. Photobiol. A* **1998**, *17*, 137. (e) Levy-Clement, C.; Tena-Zaera, R.; Ryan, M. A.; Katty, A.; Hodes, G. *Adv. Mater.* **2005**, *17*, 1512.

(8) Tennakoneb, K.; Wickramanayakab, S.; Basub, S. *Chem. Phys. Lett.* **1985**, *121*, 551.

(9) (a) Mahrov, B.; Hagfeldt, A.; Lenzmann, F.; Boschloo, G. *Sol. Energy Mater. Sol. Cells* **2005**, *88*, 351. (b) Regan, B. C. O.; Lenzmann. F. *J. Phys. Chem. B* **2004**, *108*, 4342. (c) Fernando, C. A. N.; Priyankara, W. T. C.; Dharmadasa, I. M. *Renewable Energy* **2002**, *25*, 69.

(10) (a) O'Regan, B.; Schwartz, D. T. *Chem. Mater.* **1995**, *7*, 1349. (b) Fernando, C. A. N.; Kitagawa, A.; Suzuki, M.; Takahashi, K.; Komura, T. *Sol. Energy Mater. Sol. Cells* **1994**, *33*, 301. (c) De Taccomi, N. R.; Son, Y.; Rajeshwar, K. *J. Phys. Chem.* **1993**, *97*, 1042.

(11) Sindhu, K. S.; Sekhon, S. S.; Hashmi, S. A.; Chandra, S. *Eur. Polym. J.* **1993**, *29*, 779.

(12) Zhang, H.; Marin, V.; Fijten, M. W. M.; Schubert, U. S. *J. Polym. Sci. A* **2004**, *42*, 1876.

(13) Rost, C.; Sieber, I.; Lux-Steiner, M. C.; Koenenkamp, R. *Appl. Phys. Lett.* **1999**, *75*, 692.

(14) Bringley, J. F.; Eachus, R. S.; Marchetti, A. P. *J. Phys. Chem. B* **2002**, *106*, 5346.

(15) Tacconi, N. R.; Rajeshwar, K. *Electrochim. Acta* **2002**, *47*, 2603.

(16) Yang, M.; Zhu, J.; Li, J. *Mater. Lett.* **2005**, *59*, 842.

(17) (a) Smith, D. L.; Saunders, V. J. *Acta Crystallogr. B* **1981**, *37*, 1807. (b) Smith, D. L.; Saunders, V. I. *Acta Crystallogr. B* **1982**, *38*, 907.

(18) (a) Zhang, Z.; Sun, H.; Shao, X.; Li, D.; Yu, H.; Han, M. *Adv. Mater.* **2005**, *17*, 42. (b) Sano, M.; Maruo, T.; Yamatera, H. *J. Chem. Phys.* **1988**, *89*, 1185.

(19) (a) Brown, I. D.; Altermatt, D. *Acta Crystallogr. B* **1985**, *41*, 244. (b) Brown, I. D. *Acta Crystallogr. B* **1992**, *48*, 553. (c) Urusov, V. S.; Orlov, I. P. *Crystallogr. Rep.* **1999**, *44*, 686.

(20) (a) Xu, J.; Xue, D. *J. Phys. Chem. B* **2005** *109*, 17157. (b) Yan, C.; Xue, D. *J. Phys. Chem. B* **2005**, *109*, 12358. (c) Yan, C.; Xue, D. *J. Phys. Chem. B* **2006**, *110*, 1581. (d) Xu, D.; Xue, D.; Ratajczak, H. *J. Mol. Struct.* **2005**, *740*, 37. (e) Xu, D.; Xue, D. *J. Cryst. Growth* **2006**, *286*, 108. (f) Xu, D.; Xue, D. *Phys. B* **2005**, *370*, 84.

(21) (a) Xu, J.; Xue, D.; Yan, C. *Mater. Lett.* **2005**, *59*, 2920. (b) Kormann, C.; Bahnemann, D. W.; Hoffmann. M. R. *J. Phys. Chem.* **1988**, *92*, 5196.